Tetrahedral Colloidal Clusters from Random Parking of Bidisperse Spheres

Nicholas B. Schade, Miranda C. Holmes-Cerfon, Elizabeth R. Chen, Dina Aronzon, Jesse W. Collins, Jonathan A. Fan, Federico Capasso, and Vinothan N. Manoharan

Phys. Rev. Lett. **110**, 148303 — Published 4 April 2013

DOI: 10.1103/PhysRevLett.110.148303

Tetrahedral colloidal clusters from random parking of bidisperse spheres

Nicholas B. Schade,[1] Miranda C. Holmes-Cerfon,[2] Elizabeth R. Chen,[3] Dina Aronzon,[2] Jesse W. Collins,[2] Jonathan A. Fan,[2] Federico Capasso,[2] and Vinothan N. Manoharan[2,1]

[1]*Department of Physics, Harvard University, Cambridge, Massachusetts 02138, USA*
[2]*School of Engineering and Applied Sciences, Harvard University, Cambridge, Massachusetts 02138, USA*
[3]*Department of Mathematics, University of Michigan, Ann Arbor, Michigan 48109, USA*

Using experiments and simulations, we investigate the clusters that form when colloidal spheres stick irreversibly to – or "park" on – smaller spheres. We use either oppositely charged particles or particles labeled with complementary DNA sequences, and we vary the ratio α of large to small sphere radii. Once bound, the large spheres cannot rearrange, and thus the clusters do not form dense or symmetric packings. Nevertheless, this stochastic aggregation process yields a remarkably narrow distribution of clusters with nearly 90% tetrahedra at $\alpha = 2.45$. The high yield of tetrahedra, which reaches 100% in simulations at $\alpha = 2.41$, arises not simply because of packing constraints, but also because of the existence of a long-time lower bound that we call the "minimum parking" number. We derive this lower bound from solutions to the classic mathematical problem of spherical covering, and we show that there is a critical size ratio $\alpha_c = (1 + \sqrt{2}) \approx 2.41$, close to the observed point of maximum yield, where the lower bound equals the upper bound set by packing constraints. The emergence of a critical value in a random aggregation process offers a robust method to assemble uniform clusters for a variety of applications, including metamaterials.

Understanding the geometry of clusters formed from small particles is a fundamental problem in condensed matter physics, with implications for phenomena ranging from nucleation [1] to self-assembly [2]. Colloidal particles are a useful experimental system for studying cluster geometry and its relation to phase behavior [3] for several reasons: they are large enough to be directly observed using optical microscopy; their assembly can be understood in terms of geometry [4, 5]; and they can be driven to cluster by a variety of controllable interactions, including capillary forces [2], depletion [6], fluctuation-induced forces [7], or DNA-mediated attraction [8]. Colloidal clusters are also useful materials in their own right. They can be used, for example, as building blocks for isotropic optical metamaterials known as metafluids [9–11]. Tetrahedral clusters are of particular interest for metafluids since the tetrahedron is the simplest cluster with isotropic dipolar symmetry [9]. An unsolved challenge for this application is to determine the interactions and conditions that enable assembly of bulk quantities of highly symmetric, uniform clusters such as tetrahedra.

With this motivation in mind, we study experimentally the geometry and size distribution of binary clusters formed when small colloidal spheres are mixed with an excess of large spheres that stick *irreversibly and randomly* to their surfaces (Figure 1a). An obvious way to control the cluster geometry in such binary systems is to vary the size ratio. One might expect that at certain ratios the particles could arrange into dense clusters or "spherical packings" – arrangements of spheres around a central sphere that maximize surface density [12–14]. Such packings have long been used in modeling the microstructure of dense, disordered atomic systems [15, 16]. But unlike atoms, colloidal particles can stick irreversibly, such that two particles bound to a third show no motion relative to one another. This type of binding occurs frequently in strongly interacting, monodisperse colloidal suspensions, which consequently form fractal aggregates instead of dense glasses [17, 18]. Similarly, in the binary systems we study, the irreversible and stochastic process of sticking precludes the formation of dense or symmetric packings. The large spheres *park*, rather than pack, on the surfaces of the small spheres.

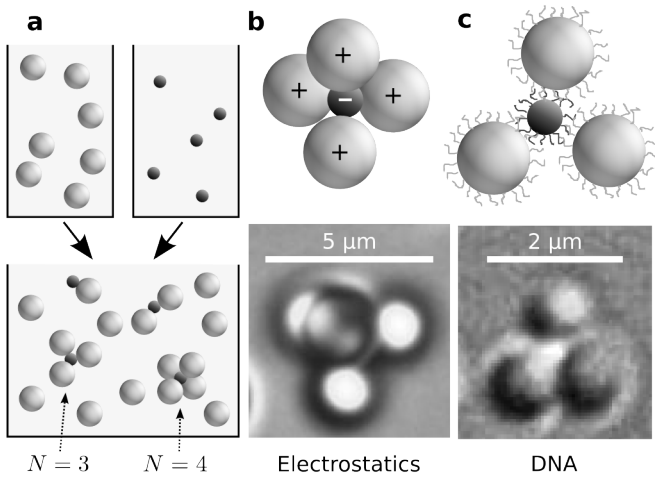

FIG. 1. (a) Two colloidal sphere species are mixed together to form clusters. (b) Oppositely charged polystyrene spheres cluster due to electrostatic attraction. Optical micrograph shows a tetramer ($N = 4$). (c) Polystyrene spheres labeled with complementary DNA strands (not to scale) cluster due to DNA hybridization. Optical micrograph shows a trimer ($N = 3$); the small, central sphere is fluorescent.

Surprisingly, this random and non-equilibrium process can produce clusters of uniform size. Our experiments show that at a size ratio $\alpha = R_{\mathrm{big}}/R_{\mathrm{small}} = 2.45$, where

Size ratio α	1.94	2.45	3.06	4.29
$N = 6$	6.3	0.0	0.0	0.0
$N = 5$	39.2	0.8	0.0	0.0
$N = 4$	54.4	90.2	18.6	0.7
$N = 3$	0.0	6.6	69.9	35.9
$N = 2$	0.0	0.8	10.9	51.0
$N = 1$	0.0	0.8	0.6	11.1
$N = 0$	0.0	0.8	0.0	1.3

TABLE I. Experimentally observed cluster size distributions for charged colloids. Percentages of total are listed. The distribution for $\alpha = 2.45$ (red) is sharply peaked at $N = 4$.

R_{big} and R_{small} are the sphere radii, nearly all of the clusters contain four large spheres stuck to a smaller sphere (Table I). In these experiments we use a 100:1 stoichiometric ratio of the two sphere species, statistically ensuring that each cluster contains only one small sphere surrounded by two or more larger spheres. After waiting several days for the average cluster size to saturate, we measure the distribution of N, the number of large spheres bound to each small sphere [19]. We do not count single large spheres, nonspecifically aggregated clusters of large spheres, or clusters with multiple small spheres. While there are many isolated large spheres due to the high stoichiometric ratio, the latter two types of cluster are rare.

The $N = 4$ tetramers that we observe are not dense packings or, in general, symmetric arrangements. As can be seen from the images in Figure 1, there is space between the large particles, and the resulting tetrahedra are irregular. Moreover, the ratio $\alpha = 2.45$ is well below the value $\alpha = 4.44$ found by Miracle *et al.* [20] for efficient tetrahedral packing in binary atomic clusters. In fact, at $\alpha = 4.29$, closer to this bound, we see much smaller clusters and few tetrahedra. The sparsity of large spheres in the clusters is a result of the irreversible, nonequilibrium, random binding: once the big particles stick to the smaller ones, we do not see them detach or move relative to one another. We expected such a stochastic process to lead to a much broader distribution of clusters. At other values of α it does (Table I), but at $\alpha = 2.45$ we obtain 90% tetramers.

The high yield of tetramers occurs in two experimental systems with different types of interactions. In both systems the interactions are specific, strong, and short-ranged, and the particles do not rearrange once bound. In the first system the clustering is driven by electrostatic interactions. We mix large, positively-charged particles with small, negatively-charged particles, as shown in Figure 1b. To adjust α, we use several different particle sizes [19]. We add salt to reduce the Debye length to approximately 3 nm, small enough to ensure that the interaction range does not significantly influence the effective particle size. In the second system the clustering is driven by hybridization of grafted DNA strands [19]. As shown in Figure 1c, we mix small and large spheres labeled with complementary DNA oligonucleotides [21]. We work well below the DNA melting temperature so that the attractive interaction is many times the thermal energy [22].

To better understand why the distribution is sharply-peaked at $N = 4$ for $\alpha = 2.45$, we use simulations and analytical techniques that account for the irreversibility of the aggregation process. Our simulations use a "random parking" algorithm [23–26] to model the formation of clusters. The algorithm involves attaching large spheres to randomly selected positions on the surface of a small sphere, subject to a no-overlap constraint [19]. We do not model the finite range of the interactions, which in both experimental systems is small compared to the particle size, or the diffusion of the particles prior to binding. In accord with experimental observations, the particles are not allowed to rearrange once bound. We repeat the process numerically to obtain distributions of cluster sizes as a function of a single parameter, α.

The simulations find a 100% yield of tetramers at the size ratio $\alpha \approx 2.41$. As in the experiments, the large particles in these tetramers are not densely packed, and the clusters are therefore distorted tetrahedra. We also find that while the yield of any particular cluster can be maximized by varying α (Figure 2a), the yield approaches 100% only for dimers ($N = 2$) and tetramers ($N = 4$). Interestingly, the yield curve for tetramers has a cusp at its peak, showing that the size ratio α_c at the maximum is a mathematical critical point.

The simulated distributions agree well with those found experimentally (Figure 2b,c) for both electrostatic and DNA-mediated interactions. For instance, at $\alpha = 2.45$ with electrostatic interactions, we find a sharply-peaked distribution consisting almost entirely of tetramers. This value of α is close to but not precisely at the critical value, so a small yield of trimers is predicted and observed experimentally. In contrast, at $\alpha = 1.90$ we find a mixture of mostly $N = 4$ and $N = 5$ clusters in both the DNA system and simulations. Some discrepancy arises between the simulated and experimental histograms because the yield curves in Figure 2a are steep; a slight error in the effective size ratio can shift the cluster distribution. Nevertheless, the random sphere parking model successfully reproduces both the large yield of tetrahedra near α_c and the details of the measured histograms at various other α.

That we can reproduce the same phenomenon in two different experimental systems and in a one-parameter model suggests that the critical size ratio α_c has a universal, geometrical origin. Intuitively one might expect that it is related to packing constraints on the large spheres. Other theoretical studies of random sphere parking [23, 24] have calculated the maximum number of large spheres N_{max} that can fit around a small sphere at a given α. However, this bound cannot by itself ex-

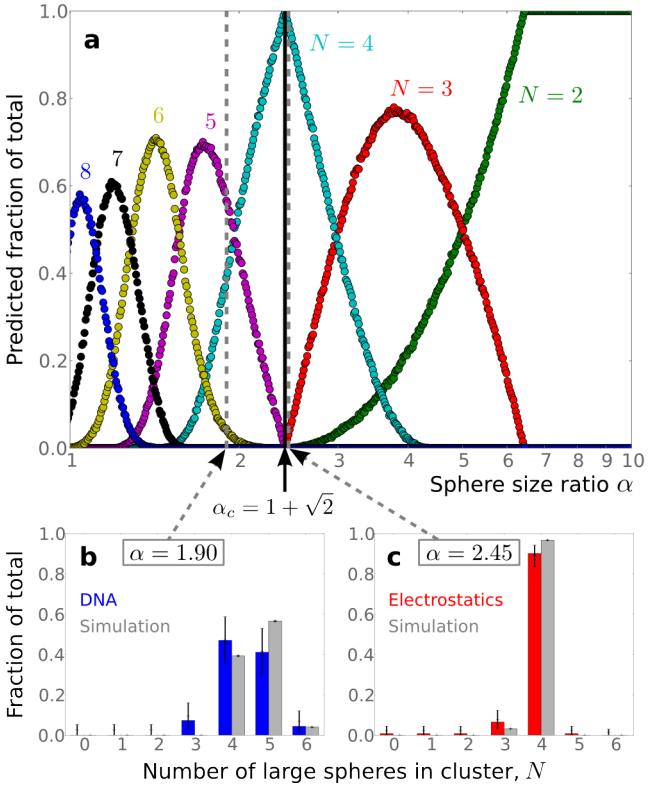

FIG. 2. (a) Yield curves, as determined by simulations, for N-particle clusters, $2 \leq N \leq 8$, where the critical size ratio α_c is marked with a black line. Below are histograms for (b) DNA-labeled particles (blue) at $\alpha = 1.90$ and (c) charged particles (red) at $\alpha = 2.45$, as observed in experiments and as predicted from simulations (gray). Error bars are 95% confidence intervals (Wilson score interval method).

plain why the yield of tetramers can reach 100% while that of other clusters, such as trimers or hexamers, cannot. At a given α, it tells us only why no clusters larger than $N_{\max}(\alpha)$ can form, but it says nothing about the probability of forming smaller clusters with different arrangements.

Therefore we also examine a different bound, one not previously discussed in the context of random sphere parking: the "minimum parking" curve $N_{\min}(\alpha)$. $N_{\min}$ is the smallest number of hard spheres that can be positioned on a smaller sphere such that another sphere cannot fit. To understand this bound, consider a simple, one-dimensional analogy to car parking on a busy city street, where if a space opens up that is large enough to fit a car, it is filled. The minimum parking number occurs when all drivers have been equally inconsiderate, leaving spaces between their parked cars that are all slightly too small for another car to fit. This lower bound is meaningful only at long times, when all available parking spaces have been filled. The long-time limit holds also for our experiments and simulations, which we carry out until the average cluster size has saturated.

Whereas the upper bound $N_{\max}(\alpha)$ is straightforwardly related to solutions of the well-known spherical packing problem [13, 27], the calculation of the lower bound $N_{\min}(\alpha)$ requires a different approach. In our clusters, the distance between the centers of any two big spheres must be at least $2R_{\text{big}}$. Consider then a sphere of radius $(R_{\text{small}} + R_{\text{big}})$ that circumscribes the centers of the parked spheres. If this sphere is completely covered with N circles of radius $2R_{\text{big}}$, it will be impossible to add an $(N+1)^{\text{th}}$ large sphere. We are led naturally to the *spherical covering* problem, a problem with a rich history in mathematics. Like spherical packings, spherical coverings are solutions to an extremum problem: they are arrangements of N points on a sphere that minimize the largest distance between any location on the sphere surface and the closest point [13]. But unlike spherical packings, spherical coverings need not correspond to arrangements of non-overlapping spheres. We therefore solve for the minimum parking curve by examining the solutions to the spherical covering problem [27] at each N and manually verifying that they correspond to non-overlapping configurations [19].

Our analytical results for the bounds reveal why α_c is a special point: it is the only non-trivial point where the calculated maximum and minimum parking curves come together (Figure 3). Analytically we find the location of the critical value to be $\alpha_c = (1 + \sqrt{2}) \approx 2.41$, very close to the values where the experimental distributions are peaked. At α slightly larger than this value, the minimum parking configuration corresponds to two spheres placed at opposite poles ($N_{\min} = 2$), and the maximum N is obtained by first parking three large spheres next to one another, so that there is room for one more sphere to park ($N_{\max} = 4$). At α slightly smaller than α_c, the big spheres can park along orthogonal axes about the small sphere to make an octahedron ($N_{\max} = 6$). The minimum N is obtained by placing four spheres as far from each other as possible, so as to make the addition of a fifth impossible ($N_{\min} = 4$). Thus as we increase α through α_c, $N_{\max}$ goes from 6 to 4 and $N_{\min}$ from 4 to 2, and the two curves become infinitesimally close.

The parking process is therefore geometrically constrained to yield clusters with exactly $N = 4$ particles in the limit $\alpha \to \alpha_c$. A simple geometric argument sheds some light on this result. At α_c there is always room for four large spheres to park. Parking more spheres requires that at least three park precisely along a great circle of the smaller particle, but the probability of this happening randomly is zero. Thus irreversible binary aggregation, a stochastic process, has a deterministic feature at the critical size ratio: although the space between the large spheres can vary, all clusters must be tetramers. Our numerical approach confirms that the statistical dispersion in the cluster size distribution vanishes at α_c, as shown in Figure 3.

The experimental and simulated distributions differ

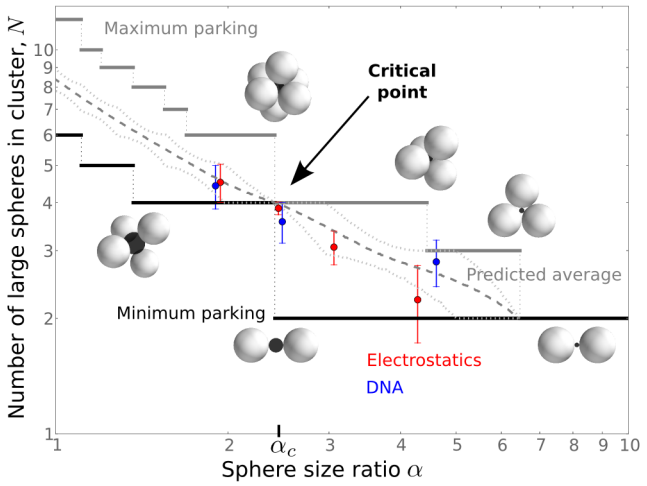

FIG. 3. $N_{\max}$ (solid gray) and $N_{\min}$ (black) as functions of α. Cluster images show sphere configurations at discontinuities of these curves. Average cluster sizes from simulations (dashed gray) and experiments (blue and red data points) are shown. We characterize the statistical dispersion in each distribution by the average absolute deviation from the median, indicated by dotted light gray lines for simulations and vertical bars for experiments.

slightly due to two effects. First, the measured sizes tend to be smaller than the simulated ones because a few parking spaces remain unfilled even at long times. This effect is more pronounced for larger spheres, which diffuse more slowly and encounter the small spheres less frequently. The systems most affected are the electrostatic ones at $\alpha = 3.06$ and 4.29. Second, the experimental size ratios can vary by 5% due to polydispersity. Both of these factors increase the width in the experimental distributions and diminish the achievable yield of tetramers near α_c. The random parking model also assumes the interactions are infinitesimally short-ranged and isotropic. It would not be valid if, for example, there were surface inhomogeneities on length scales comparable to the particle radii. Nevertheless, the experimental data indicate that near α_c a tetramer yield of at least 90% is possible, and the model is useful for predicting cluster size distributions in two very different colloidal systems.

These results have both fundamental and practical consequences. On the fundamental side, the particle size ratio could affect the jamming threshold in bulk packings of bidisperse spheres. Previous simulations of these systems have shown that the distribution of coordination numbers also depends on the size ratio [28] and may be modeled using random parking [25]. This contrasts with dense atomic systems like metallic glasses [15, 16] in which the atoms have some freedom to rearrange locally. In these systems packing constraints may explain structure and coordination better than parking arguments.

On the practical side, this random aggregation process is a simple way to mass produce tetrahedral clusters in theoretically 100% yield. Although the tetrahedra we produce are irregular in that the distance between the large spheres can vary, it may well be possible to form large quantities of symmetric tetrahedra simply by shrinking the small spheres after the tetramers have formed [29]. An additional step, such as density gradient centrifugation [2], will also be required to separate the assembled clusters from the many unbound large particles. Furthermore, although the yield will approach 100% only for dimers and tetramers, the yield of any N-particle cluster can be maximized by choosing the appropriate size ratio. For instance, the yield of octahedral clusters, also promising candidates for building metamaterials [10], may surpass 70% at $\alpha = 1.42$.

The size ratio in binary colloidal systems thus emerges as a valuable control parameter for directed self-assembly. Moreover, because it does not require precise control over the interactions, random parking offers a robust and simple way to make colloidal clusters that are more monodisperse than those prepared through other methods [2].

We thank W. Benjamin Rogers, Rodrigo Guerra and Michael P. Brenner for helpful discussions. This work was funded by the National Science Foundation NIRT program (grant no. ECCS-0709323) and the Harvard MRSEC (grant no. DMR-0820484). NBS acknowledges support from the Department of Energy Office of Science Graduate Fellowship Program, administered by ORISE-ORAU under contract no. DE-AC05-06OR23100.

[1] K. F. Kelton, G. W. Lee, A. K. Gangopadhyay, R. W. Hyers, T. J. Rathz, J. R. Rogers, M. B. Robinson, and D. S. Robinson, Phys. Rev. Lett. **90**, 195504 (2003).
[2] V. N. Manoharan, M. T. Elsesser, and D. J. Pine, Science **301**, 483 (2003).
[3] U. Gasser, E. R. Weeks, A. Schofield, P. N. Pusey, and D. A. Weitz, Science **292**, 258 (2001).
[4] N. Arkus, V. N. Manoharan, and M. P. Brenner, Phys. Rev. Lett. **103**, 118303 (2009).
[5] R. S. Hoy and C. S. O'Hern, Phys. Rev. Lett. **105**, 068001 (2010).
[6] G. Meng, N. Arkus, M. P. Brenner, and V. N. Manoharan, Science **327**, 560 (2010).
[7] P. J. Yunker, K. Chen, Z. Zhang, W. G. Ellenbroek, A. J. Liu, and A. G. Yodh, Phys. Rev. E **83**, 011403 (2011).
[8] C. M. Soto, A. Srinivasan, and B. R. Ratna, J. Am. Chem. Soc. **124**, 8508 (2002).
[9] Y. A. Urzhumov, G. Shvets, J. A. Fan, F. Capasso, D. Brandl, and P. Nordlander, Opt. Express **15**, 14129 (2007).
[10] A. Alù and N. Engheta, Opt. Express **17**, 5723 (2009).
[11] J. A. Fan, C. Wu, K. Bao, J. Bao, R. Bardhan, N. J. Halas, V. N. Manoharan, P. Nordlander, G. Shvets, and F. Capasso, Science **328**, 1135 (2010).
[12] T. W. Melnyk, O. Knop, and W. R. Smith, Can. J. Chem. **55**, 1745 (1977).

[13] J. H. Conway and N. J. A. Sloane, *Sphere Packings, Lattices and Groups* (Springer-Verlag, New York, 1993).
[14] C. L. Phillips, E. Jankowski, M. Marval, and S. C. Glotzer, Phys. Rev. E **86**, 041124 (2012).
[15] T. Egami, Materials Science and Engineering: A **226228**, 261 (1997).
[16] D. B. Miracle, Nat. Mat. **3**, 697 (2004).
[17] D. A. Weitz and M. Oliveria, Phys. Rev. Lett. **52**, 1433 (1984).
[18] M. Y. Lin, H. M. Lindsay, D. A. Weitz, R. C. Ball, R. Klein, and P. Meakin, Nature **339**, 360 (1989).
[19] See Supplementary Information for additional details.
[20] D. B. Miracle, W. S. Sanders, and O. N. Senkov, Phil. Mag. **83**, 2409 (2003).
[21] R. Dreyfus, M. E. Leunissen, R. Sha, A. V. Tkachenko, N. C. Seeman, D. J. Pine, and P. M. Chaikin, Phys. Rev. Lett. **102**, 048301 (2009).
[22] R. Dreyfus, M. E. Leunissen, R. Sha, A. Tkachenko, N. C. Seeman, D. J. Pine, and P. M. Chaikin, Phys. Rev. E **81**, 041404 (2010).
[23] M. L. Mansfield, L. Rakesh, and D. A. Tomalia, J. Chem. Phys. **105**, 3245 (1996).
[24] L. A. Rosen, N. A. Seaton, and E. D. Glandt, J. Chem. Phys. **85**, 7359 (1986).
[25] A. Wouterse, M. Plapp, and A. P. Philipse, J. Chem. Phys. **123** (2005).
[26] J. Talbot, G. Tarjus, P. R. V. Tassel, and P. Viot, Colloids and Surfaces A: Physicochem. Eng. Aspects **165**, 287 (2000).
[27] N. J. A. Sloane, R. H. Hardin, and W. D. Smith, "Tables of spherical codes," Published electronically at www.research.att.com/∼njas/packings/ (2011).
[28] D. He, N. N. Ekere, and L. Cai, Phys. Rev. E **60**, 7098 (1999).
[29] L. A. Lyon, J. D. Debord, S. B. Debord, C. D. Jones, J. G. McGrath, and M. J. Serpe, J. Phys. Chem. B **108**, 19099 (2004).